

## Vortex-sink dynamics

A. E. Novikov and E. A. Novikov

*Institute for Nonlinear Science, University of California, San Diego, La Jolla, California 92093-0402*

(Received 27 November 1995; revised manuscript received 24 May 1996)

Interaction of a point vortex sink (twister) with an obstacle in a stationary and nonstationary flow is considered. Classification of twister trajectories, depending on nondimensional parameters of the system, and the probability of twister-obstacle collisions are presented. Equations for the screened (Besselian) twisters are presented and some solutions of these equations are discussed. More general situations and applications, including screened twisters in a superconductor, are also discussed. [S1063-651X(96)07410-7]

PACS number(s): 47.32.-y

### I. INTRODUCTION

A characteristic feature of quasilinear vortices of various kinds is the convergent radial motion of the medium at the base of such a vortex. Good examples are the sink vortices in bathtubs, whirlwinds, tornadoes, and typhoons. The convergence in such vortices can be simulated by means of sinks (whose physical nature is not considered; in case of typhoons we have convection above the surface of the ocean). The problem is then reduced to the two-dimensional hydrodynamics [1].

A simple model in such an approach is a combination of a point vortex and sink, which is called a helical vortex (from the shape of streamlines). We will use a shorter name: *twister*. We will show first that twisters have a natural attraction to any obstacle [depending on a scale of phenomena, it can be a change in a relief, a man-made structure, or a tree: one of the authors (E.N.) witnessed a relatively thin dust devil hitting a tree]. Next we will present classification of twister trajectories in a stationary flow for a variety of non-dimensional parameters of the system. Then we will calculate probabilities of twister-obstacle collisions in a non-stationary flow. Finally, we will turn to a more general family of animals (*screened twisters*) in the context of various applications.

### II. ORDINARY TWISTERS

Consider a twister with the vortex intensity  $\kappa$  (for  $\kappa > 0$  we assume counterclockwise rotation of fluid). The source (sink) intensity is  $\mu$  (a sink corresponds to  $\mu < 0$ ). As an obstacle we choose a cylinder with the radius  $a$ . For a motion of ideal fluid, we must ensure a zero normal component of the velocity at the surface of a body (generally, in the frame of reference moving with the body, if it is moving, like a car or a ship). For an ordinary vortex this condition is enforced by an image vortex placed inside the cylinder at the distance from the center  $a^2/r$ , where  $r$  corresponds to the position of the original twister. It is well known from vortex dynamics that the intensity of the image vortex is  $-\kappa$  (which has opposite sign). However, it is easy to see, in particular for the case of a flat boundary, that the intensity of image source or sink is  $\mu$ , which has the same sign as for the original twister. This causes a fatal attraction of twisters to any obstacles (not only cylindrical or flat). In the case of a

cylindrical boundary we have to place at the center of the cylinder an additional source or sink with intensity  $-\mu$  (which has opposite sign) [2]. The case of a flat boundary and screened twister is presented in Sec. III.

Consider external flow with oscillating fluid velocity at infinity

$$u(t) = u_0(1 + \epsilon \sin \omega t), \quad (1)$$

where  $\epsilon$  is the nondimensional amplitude of the oscillation and  $\omega$  is the frequency. In the plane of motion the flow is assumed from top to bottom. The corresponding potential motion of the fluid around the cylinder is represented by a dipole (see, for example, Ref. [3]).

In polar coordinates  $(r, \phi)$  with the origin in the center of the cylinder and with additional circulation  $\kappa_0$  around the cylinder, the equations of motion for the twister have the form

$$\frac{dr}{dt} = \frac{\mu a^2}{2\pi r(r^2 - a^2)} - u_0(1 + \epsilon \sin \omega t)(1 - a^2 r^{-2}) \sin \phi, \quad (2)$$

$$r \frac{d\phi}{dt} = -\frac{\kappa r}{2\pi(r^2 - a^2)} + \frac{\kappa_0}{2\pi r} - u_0(1 + \epsilon \sin \omega t)(1 + a^2 r^{-2}) \cos \phi. \quad (3)$$

For an ordinary vortex (with  $\mu = 0$ ) these equations were investigated in Refs. [4,5] and chaotic behavior was discovered.

In the absence of external flow ( $u_0 = 0$ ), we obtain, from Eq. (2),

$$\frac{1}{3a} (r^3 - r_0^3) - \frac{1}{2} (r^2 - r_0^2) = \mu t / 2\pi, \quad (4)$$

where  $r_0$  is the initial distance of twister from the center of the cylinder ( $r_0 > a$ ). We see that for an arbitrary initial position, the twister will hit the surface of the cylinder ( $r = a$ ) in a finite time, given by (4).

From (2) and (3), with  $u_0 = 0$ , we have

$$\phi - \phi_0 = \frac{\kappa_0 - \kappa}{\mu} \ln(r/r_0) + \frac{\kappa_0 a^2}{2\mu} (r^{-2} - r_0^{-2}), \quad (5)$$

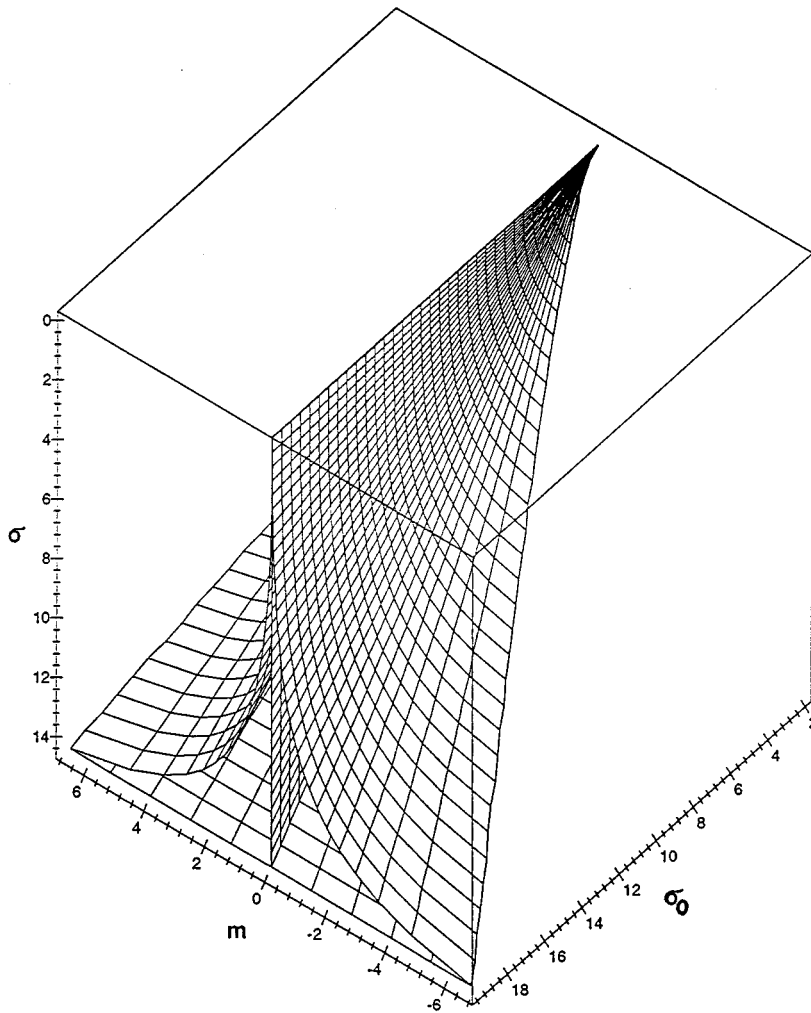


FIG. 1. Classification of twister trajectories in the parameter space: inside the funnel, two saddle points and focus; outside, one saddle point (see the text).

where  $\phi_0$  is the initial angle. Equations (4) and (5) give the whole trajectory of the twister. The place of collision is determined by (5) with  $r = a$ .

For stationary external flow ( $u_0 \neq 0, \epsilon = 0$ ) we will have an area of initial conditions from which trajectories will hit the cylinder. Other trajectories will go away. The corresponding separatrices will generally depend on three nondimensional parameters  $\sigma = \kappa/2 \pi u_0 a$ ,  $\sigma_0 = \kappa_0/2 \pi u_0 a$ , and  $m = \mu/2 \pi u_0 a$ . In particular, for a pure sink ( $\sigma = \sigma_0 = 0, m < 0$ ) with  $\phi_0 = -\pi/2$ , the collisions occur only under the condition

$$|m| > (r_0^2 - a^2)^2 r_0^{-1} a^{-3}, \tag{6}$$

which follows from (2).

In order to study trajectories and separatrices systematically, we have to find first stationary points of the system (2) and (3) with  $\epsilon = 0$ . By putting zero on the left-hand sides of these equations and excluding  $\phi$ , we get the algebraic equation

$$m^2 z(z+1)^2 + z(z-1)^2 [\sigma_0(z-1) + \sigma z]^2 = (z-1)^2 (z^2 - 1)^2, \tag{7}$$

where  $z = \rho^2, \rho = r/a$ , and we consider  $\rho > 1$ . Having  $\rho$ , we can find  $\phi$  from (2) or (3). Numerical analysis of Eq. (7) with the condition  $z > 1$  shows that, depending on the values of the

parameters  $m, \sigma$ , and  $\sigma_0$ , this equation has from one to three real roots. Figure 1 summarizes these data. Inside the indicated three-dimensional area in the parameter space we have three roots; outside we have one root and on the boundary two roots. The cross section with  $m = 0$  corresponds to the case considered in [4,5]. Figure 2 presents a cross section of the parameter space with  $\sigma_0 = 11$ .

Linearization of the system (2) and (3) in the vicinity of a stationary point shows that in the case of one root we have a saddle (hyperbolic) point and in the case of three roots we have two saddle points and one focus (spiral). For  $m > 0$  the focus is stable and for  $m < 0$  it is unstable. For  $m = 0$  instead of a focus we have an elliptic point [4,5]. On the boundary in the parameter space one of the saddle points and the focus merge into a node.

Let us note that the right boundary in Fig. 2 is curved. It is more clear in Fig. 3, where positions of stationary points are presented for  $\sigma_0 = 11$ , discrete values of  $\sigma$ , and continuous changes of  $m$  from  $-100$  to  $100$ .

Consider the case with  $\sigma = 6.85$ , where we have four intersections with the curved right boundary in Fig. 2. This case corresponds to curve 3 in Fig. 3. For  $m < m_1 = -3.08$  we have one saddle point. For  $m = m_1$  (first intersection) an additional node appears (indicated by an asterisk), which then splits into a focus and a second saddle point. The fat piece of curve corresponds to the coexistence of three stationary

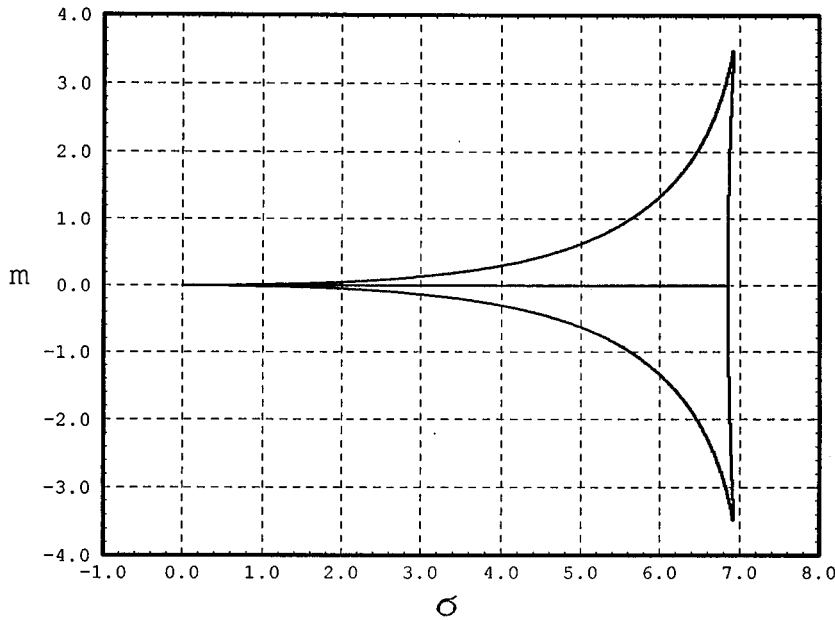


FIG. 2. Cross section of Fig. 1 with  $\sigma_0=11$ .

points. For  $m=m_2=-1.08$  (second intersection) the focus and the first saddle point merge into a node (indicated by a circle) and then disappear. For  $-m_2 > m > m_2$  we have only one (second) saddle point. For  $m > 0$  we have two more intersections and the same events in reverse order.

For  $\sigma=6$  (curve 4 in Fig. 3) and  $\sigma=4$  (curve 5) we have only two intersections and the corresponding curves consist of loops (focus and second saddle, between intersections) and separate lines (first saddle). For  $\sigma=11$  (curve 1) and  $\sigma=9$  (curve 2) there is no intersection and only one saddle point.

Twister trajectories for the case of one saddle point and  $\sigma, \sigma_0 > 0$  are presented in Fig. 4. Fat lines indicate separatrices. Figure 5 presents the case with one saddle point and  $\sigma > 0, \sigma_0 < 0$ . A more complex situation with two saddle points and one unstable focus is presented in Fig. 6. A series of twister trajectories with the same starting point and different values of parameter  $m$  are depicted in Fig. 7.

For nonstationary external flow ( $\epsilon \neq 0$ ) there are no fixed separatrices and the twister trajectory depends additionally on the phase of the oscillating flow. Denote a discrete phase by  $\alpha_k = 2\pi k/n$ , where  $k=0, \dots, n-1$  and  $n$  is the number of different phases. We add  $\alpha_k$  to the argument  $\omega t$  of the oscillations in Eqs. (2) and (3) and consider a family of trajectories with different initial phases. The probability of a twister-body collision  $P$  for a fixed initial position is naturally defined as the number of trajectories hitting the body, divided by the total number of trajectories  $n$ . Figure 8 presents two families of trajectories with initial positions on two stationary separatrices and  $n=20$ . The dependence of the probability on the position along the horizontal line intersecting stationary separatrices is depicted in Fig. 9. This figure is obtained with  $n=10^3$  for each of the  $10^3$  initial points. We see that probability changes sharply when approaching 0 and 1. In the case of small  $\epsilon$ , the limiting points are determined by the stationary separatrices, corresponding to external

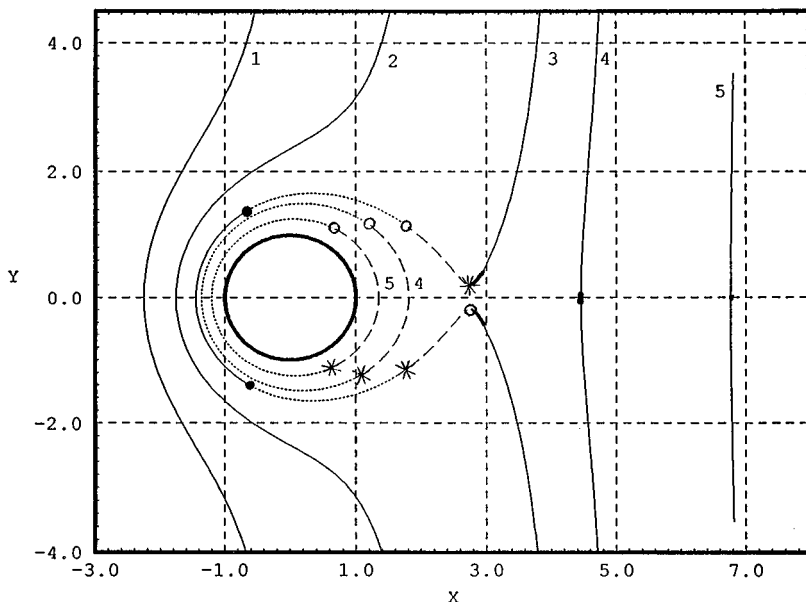


FIG. 3. Positions of stationary points ( $\sigma_0=11$  and  $100 > m > -100$ ): curves 1–5 correspond to  $\sigma=11, 9, 6.85, 6, 4$  and dashed curve indicates the focus (see the text).

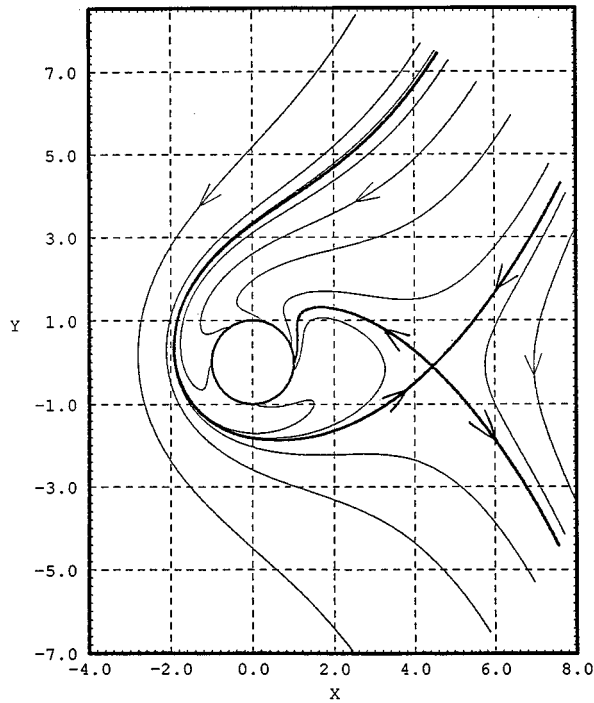


FIG. 4. Twister trajectories with one saddle point ( $\sigma_0=11$ ,  $\sigma=6$ , and  $m=-2$ ). Fat lines indicate separatrices.

flows with velocities  $U_0(1 \pm \epsilon)$ .

Let us note that for  $m \neq 0$ , the system (2) and (3) is generally non-Hamiltonian. The system of twisters (without obstacle) with equal ratios of the sink and vortex intensities is Hamiltonian [1]. Quasilinear vortices with a finite core can be approximated by a system of point twisters. Obstacles of various shapes can be considered by using the corresponding Green's functions.

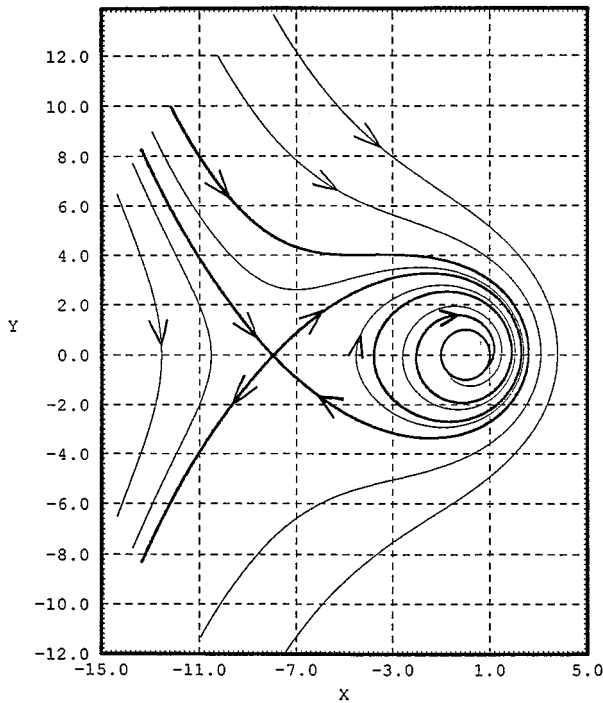


FIG. 5. Same as in Fig. 4, but with  $\sigma_0=-2$ .

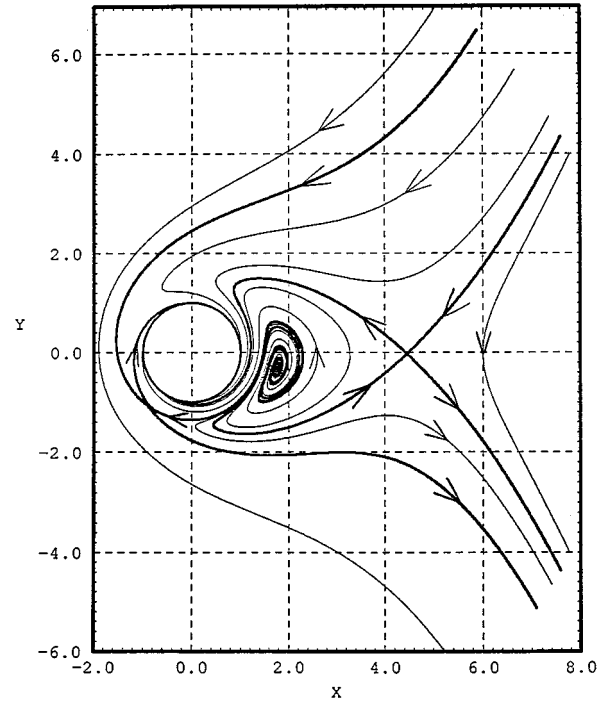


FIG. 6. Twister trajectories with two saddle points and focus ( $\sigma_0=11$ ,  $\sigma=6$ , and  $m=-0.5$ ).

### III. SCREENED TWISTERS

Twisters could find applications not only in the cases mentioned above, but also in other fields of science, just as ordinary linear and screened (Besselian) vortices are important objects of investigation in the theory of superfluidity, superconductivity, and magnetized plasma [6,7]. In particular, it was suggested [7] that the dynamics of vortices in a superconductor of a second kind, as well as a finite-dimensional model of magnetized plasma, can be described by the Hamiltonian system

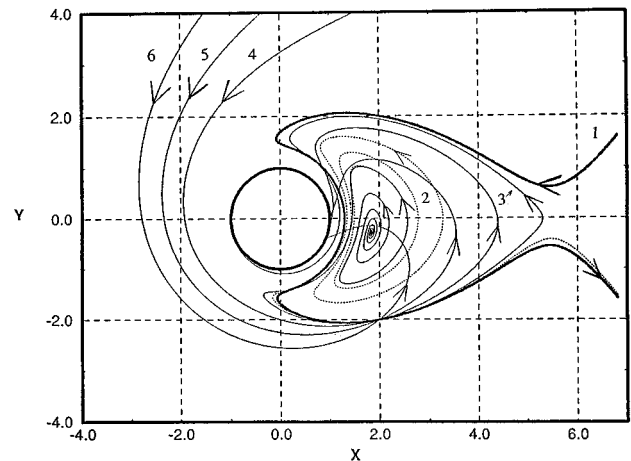


FIG. 7. Twister trajectories with a common point,  $\sigma_0=15$  and  $\sigma=9$ . Curve 1 ( $m=0$ ), twister is moving from  $\infty$  to  $\infty$ ; dotted curve 2 ( $m=-0.2$ ), from the focus (which is not shown) to  $\infty$ ; curve 3 ( $m=-0.5$ ), from the focus to the body; curves 4-6, from  $\infty$  to the body.

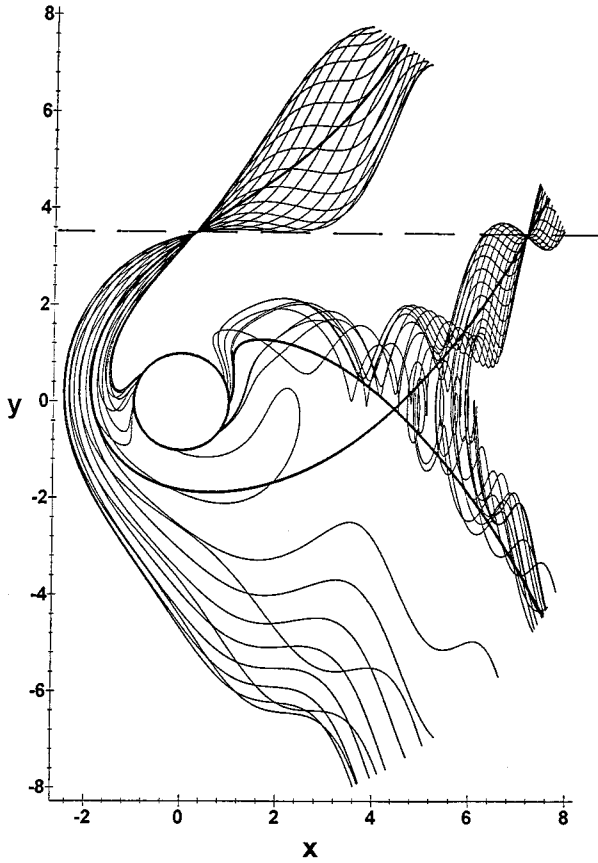


FIG. 8. Nonstationary twister trajectories ( $\sigma_0=11$ ,  $\sigma=6$ ,  $m=-2$ ,  $\epsilon=0.7$ ,  $\omega=1$ , and  $n=20$ ) intersecting stationary separatrixes at  $y_0=3.5$  (see the text).

$$\kappa_\alpha \frac{dx_\alpha}{dt} = \frac{\partial H}{\partial y_\alpha}, \quad \kappa_\alpha \frac{dy_\alpha}{dt} = -\frac{\partial H}{\partial x_\alpha}, \quad (8)$$

$$H = \frac{1}{2\pi} \sum_{\alpha < \beta} \kappa_\alpha \kappa_\beta K_0(l_{\alpha\beta}/L),$$

$$l_{\alpha\beta} = [(x_\alpha - x_\beta)^2 + (y_\alpha - y_\beta)^2]^{1/2}. \quad (9)$$

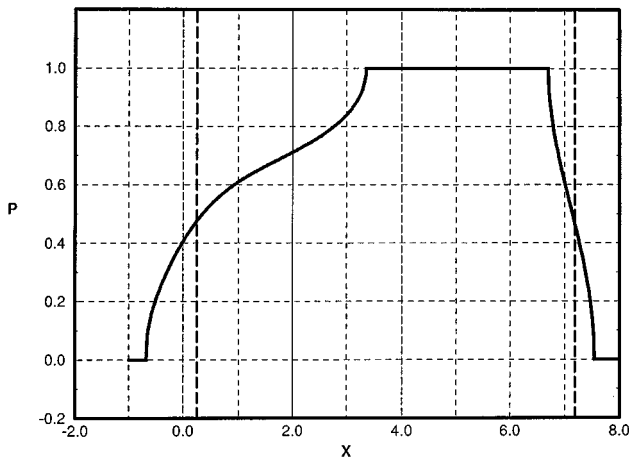


FIG. 9. Probability of a twister-body collision with the same parameters as in Fig. 8, but with  $n=10^3$ , calculated for  $10^3$  initial points (see the text).

Here  $\kappa_\alpha$  and  $(x_\alpha, y_\alpha)$  are the intensity and Cartesian coordinates of the vortices, respectively, and  $K_0$  is the Bessel function of the imaginary argument. The Hamiltonian (9) corresponds to an unbounded domain. The scale  $L$  for the superconductor is the London penetration depth [6,8]; the corresponding scale for the plasma is the effective Larmor radius of ions (calculated from the electron temperature) [9]. In the geophysical hydrodynamics the appropriate scale is the Rossby deformation radius [10]. It is always amazing when several quite different physical phenomena are described by the same equations.

The function  $K_0$  has asymptotes

$$K_0(\rho) \approx -C + \ln 2 - \ln \rho, \quad \rho \ll 1, \quad (10)$$

$$K_0 \approx (\pi/2\rho)^{1/2} e^{-\rho}, \quad \rho \gg 1, \quad (11)$$

where  $C \approx 0.577$  is the Euler constant. If all the distances between vortices are far smaller than  $L$ , then all the results derived for ordinary vortices are applicable to screened vortices as well. If the distances between the vortices are greater than  $L$ , then the vortices (or a group of vortices) interact weakly; thus the term *screened vortex* came into being. The interaction and the collapse of a system of three screened vortices were considered in Ref. [7].

Now consider *screened twistors* by introducing sinks (sources). For the vortex in a superconductor we can imagine phenomenologically that there is some sort of convection in the core of such a vortex that creates an attraction to a boundary or to a defect. The equations for screened twistors are a generalization of (8) with an additional potential

$$\frac{dx_\alpha}{dt} = \frac{1}{\kappa_\alpha} \frac{\partial H}{\partial y_\alpha} + \frac{1}{\mu_\alpha} \frac{\partial \Phi}{\partial x_\alpha}, \quad \frac{dy_\alpha}{dt} = -\frac{1}{\kappa_\alpha} \frac{\partial H}{\partial x_\alpha} + \frac{1}{\mu_\alpha} \frac{\partial \Phi}{\partial y_\alpha}, \quad (12)$$

$$\Phi = -\frac{1}{2\pi} \sum_{\alpha < \beta} \mu_\alpha \mu_\beta K_0(l_{\alpha\beta}/L_s), \quad (13)$$

where  $\mu_\alpha$  are sink (source) intensities. The screening scale  $L_s$  for sinks (sources) generally can be different from  $L$ . For  $l_{\alpha\beta} \ll \min(L, L_s)$  we return to ordinary twistors. For the interaction of two screened twistors we obtain from (12), (13), and (9)

$$\frac{dl}{dt} = \frac{\mu_*}{2\pi L_s} K_1(l/L_s), \quad \mu_* = \mu_1 + \mu_2, \quad K_1(\rho) = -K_0'(\rho), \quad (14)$$

$$l \frac{d\theta}{dt} = -\frac{\kappa_*}{2\pi L} K_1(l/L), \quad \kappa_* = \kappa_1 + \kappa_2,$$

$$\theta = \arctan\left(\frac{y_1 - y_2}{x_1 - x_2}\right), \quad (15)$$

where  $l$  is the distance between twistors. This system is obviously integrable. It follows that for  $\mu_* = 0$  the distance between the screened vortices does not change, for  $\mu_* > 0$  they move apart, while for  $\mu_* < 0$  they approach each other in a finite time

$$T = -\frac{2\pi L_s^2}{\mu_*} \int_0^{l_0/L_s} \frac{d\rho}{K_1(\rho)}, \quad (16)$$

where  $l_0$  is the initial distance. Further, for  $\kappa_* = 0$  the vector distance between vortices preserves its direction, for  $\kappa_* < 0$  the vortices rotate clockwise, and for  $\kappa_* > 0$  the vortices rotate counterclockwise. Knowing the relative motion from (14) and (15), we can readily calculate the absolute motion of screened twistors using Eqs. (12) (compare with the similar analysis of ordinary twistors [1]). The interaction of the screened twister with a boundary can also be calculated similarly to the case of ordinary twistors. In particular, the attraction of a screened twister to a flat boundary is described by (14) and (15) with  $l = 2y$ , where  $y$  is the distance from the boundary, and with  $\mu_2 = \mu_1$ ,  $\kappa_2 = -\kappa_1$ , where the index 2 refers to the image screened twister. Absolute motion includes the component of velocity  $v = (\kappa_1/2\pi L)K_1(l/L)$ , parallel to the boundary.

From the simple analytical and numerical solutions presented we can see that the twister dynamics is a rich field that deserves further exploration. The classical vortex dynamics is a particular case of twister dynamics when sink intensities are zero and all distances are much smaller than  $\min(L, L_s)$ .

#### IV. CONCLUDING REMARKS

After this paper was prepared for publication, we become aware of recent work [11] in which it was concluded that vortices in a superconductor have a tendency of mutual at-

traction (repulsion) rather than simple rotation. This supports the idea that sinks (sources) can play an important role in the description of such vortices. Moreover, the asymptotic analysis [12] of the Ginzburg-Landau model [6] leads to the potential, similar to (13), where  $L_s$  equals the London penetration depth. As far as we know, the full system [(12), (9), and (13)] has not been studied before.

We also became aware of earlier works on ordinary vortex sink [13,14]. In particular, in Ref. [14] the fluid motion around an immobile vortex sink was considered and it was indicated that the influence of a cylindrical body on fluid motion is negligible for large distances because of the dipole character of this influence (in comparison with the monopole vortex sink). The motion of the vortex sink, induced by the presence of a boundary, was not considered in these works. We would like also to indicate Refs. [15,16] in which a source was used for a description of jet flows. The main goal of the present work was to bring the attention of the scientific community to the rich dynamics of the simple systems of ordinary and screened twistors with expected applications in various fields of contemporary physics.

#### ACKNOWLEDGMENTS

This work was supported by the U.S. Department of Energy under Grant No. DE-FG03-91ER14188 and by the Office of Naval Research under Grants Nos. ONR-N000-14-92-I-1610 and ONR-14-94-1-0040.

- 
- [1] E. A. Novikov and Yu. B. Sedov, *Izv. Akad. Nauk SSSR Mekh. Zhidk. Gasa* No. 1, 15 (1983) [*Fluid Dyn.* **18**, 6 (1983)].
- [2] H. Lamb, *Hydrodynamics* (Cambridge University Press, Cambridge, 1993), p. 71.
- [3] L. D. Landau and E. M. Lifshitz, *Fluid Mechanics* (Pergamon, Oxford, 1959), p. 26.
- [4] E. A. Novikov, *Phys. Lett. A* **152**, 393 (1991).
- [5] J. B. Kadtko and E. A. Novikov, *Chaos* **3**, 543 (1993).
- [6] E. M. Lifshitz and L. P. Pitaevsky, *Statistical Physics* (Pergamon, New York, 1986).
- [7] E. A. Novikov, *Ann. N. Y. Acad. Sci.* **357**, 47 (1980).
- [8] A. A. Abrikosov, *Zh. Eksp. Teor. Fiz.* **5**, 1174 (1957).
- [9] A. Hasegava and K. Mima, *Phys. Fluids* **21**, 87 (1978).
- [10] J. Pedlosky, *Geophysical Fluid Dynamics* (Springer, Berlin, 1979).
- [11] S. J. Chapman and G. Richardson, *SIAM J. Appl. Math.* **55**, 1275 (1995).
- [12] L. Peres and J. Rubinstein, *Physica D* **64**, 299 (1993).
- [13] D. Kitao, *Beitrage zur Theorie der Bewegung der Erdatmosphere und der Wirbelstürme* (Tokio University, Tokio, 1895).
- [14] A. Masotti, *Note Idrodinamiche* (Societa Editrice "Unita e pensiero," Milano, 1935).
- [15] M. Goldshtik, F. H. Hussain, and V. Shtern, *J. Fluid Mech.* **232**, 521 (1991).
- [16] V. Shtern and F. Hussain, *J. Fluid Mech.* **256**, 535 (1993).